Temporal characterization of electroencephalogram slowing activity types

Shaurya Sharma[1], David Zhou[2], Devesh Sharma[1]

[1] San Juan Hills High School, San Juan Capistrano, California, United States of America

[2] Brown University, Providence, Rhode Island, United States of America

SUMMARY

Life-threatening diseases often remain undetected until irreversible consequences manifest. EEG (electroencephalogram; electrical activity in the brain) slowing, a common phenomenon in diseases like epilepsy and dementia, also appears in other critical conditions. In this study, we analyzed data samples from the Temple University Hospital dataset — comprised of a large general population — of EEG slowing to discern distinct characteristics. We hypothesized that we would identify distinct slowing characteristics and patterns in EEG data, identified through various analysis methods showing that detection and categorization of these patterns may serve as crucial indicators for the early detection of life-threatening diseases. We identified characteristics such as generalized or focal slowing and classified them into three categories. Through time-frequency analysis, frequency-domain clustering, time-domain clustering, and additional frequency analysis methods, we explored variations in EEG slowing patterns. Our findings indicate that computational analysis using K-Means clustering, UMAP, and t-distributed Stochastic Neighbor Embedding (t-SNE) algorithms against EEG data is able to identify distinct slowing patterns, suggesting that EEG features could be used for early detection and be pivotal in early intervention and prevention treatment strategies, thus confirming our hypothesis. This study highlights the critical features of EEG slowing and how these features correlate to specific types of slowing, suggesting a promising path toward new insights into disease-prevention mechanisms and further insights into disease etiology. A comprehensive understanding of the temporal aspects of EEG slowing may lead to further insights into the etiology of these diseases and facilitate future discoveries.

INTRODUCTION

Many individuals suffer from life-threatening diseases, such as Alzheimer's, Parkinson's, and epilepsy (1). These diseases are often difficult to diagnose due to external factors, such as technological limitations or limited knowledge. It can be challenging to assess disease progression or develop cures without a full understanding of the disease. These diseases can be life-threatening, and although they have a variety of causes, they share one distinct factor: they are all related to the concept of electroencephalogram (EEG) slowing (2). EEG measures the summed electrical activity of neurons in the brain (3). EEG features vary from person to person, from differential quantitative values to various shapes in the wavelengths (4). Quantitative EEG (qEEG), defined as the quantifying of EEG signatures by computational analysis, can be used to identify hallmarks of diseases and may be utilized to understand various diseases that present with EEG slowing, such as dementia or epilepsy. Studies have shown that specific quantitative EEG measures have been detected in such diseases, yet no study has precisely measured the correlation between these quantitative EEG characteristics and specific EEG slowing types, which is considered an EEG characteristic (5). While regular EEG readings generally record electrical activity or brainwaves that are representative of underlying cortical brain activity, quantitative EEG (qEEG) utilizes mathematical and statistical analysis (6). EEG slowing is known as an "abnormal" reading in the brain, whether it is in the form of waveforms or frequency; it is typically recorded in the form of increased delta and theta wave activity across different brain regions (7). There are distinct types of EEG slowing types, including but not limited to Diffuse (generalized) slowing, focal slowing, and triphasic — abnormal EEG waveform — slowing. Diffuse slowing, oftentimes attributed to background slowing, typically occurs as a side effect of plausible medication usage, while focal and triphasic are generally severe abnormal EEG readings that are associated with some type of degenerative disease (7). While EEG slowing is sometimes found in typical cases, such as sleeping or blinking, other times it is found in dangerous and life-threatening cases, including Alzheimer's, Parkinson's, and epilepsy (8). Diseases like epilepsy contain some trace of EEG slowing, which can often be detected early if EEGs are performed (9).

The onset of these diseases can occur at any age, although it is more evident in individuals classified as "elderly" or above the age of 65 (1). Particularly in patients over the age of 65, isolated or intermittent temporal slow waves — demonstrated in overall EEG slowing — are observed (2). The basic understanding of such diseases as epilepsy is constantly being studied.

Electroencephalography is useful for understanding the neurophysiological mechanisms behind diseases (10). Using machine learning algorithms and data science techniques, qEEG, and other EEG techniques can be optimized to understand these diseases and discover further findings.

Machine learning is designed to provide computers with the ability to perform tasks and learn without being explicitly coded to do so — typically coupled with artificial intelligence (11). Whether it is used for prediction models or sorting databases, machine learning increases the accuracy and efficiency of difficult problems in order to yield valuable

results. In the past, machine learning has been used for early detection schemes in the field of medicine and for processing and analyzing large sums of data. For example, deep learning — a subset of machine learning — has been designed to predict motion using brain waves (12). In this study, we specifically used an unsupervised algorithm to cluster our data into distinctive clusters to visualize the different EEG slowing types. Specifically, we utilized the following three algorithms to determine the most accurate and precise one: K-Means clustering, Uniform Manifold Approximation and Projection for Dimension Reduction (UMAP), and t-distributed Stochastic Neighbor Embedding (t-SNE). All algorithms tested are designated for clustering. To our knowledge, there have been few studies on the temporal characterization of EEG slowing.

Here, we aimed to characterize EEG slowing and assist in EEG classification. In this study, we have limited the classification to the following slowing types: (1) Diffuse (generalized) slowing, (2) focal slowing, (3) postical-abnormal EEG waveforms, specifically found in seizures; a form of focal slowing, and (4) triphasic-abnormal EEG waveforms slowing. To test machine learning characterization methods for EEG characterization, we utilized an open EEG dataset provided by Temple University with hundreds of different observations and isolated temporal patterns within the different types of EEG slowing (13). We hypothesized that we could detect temporal and quantitative changes in EEG patterns and correlate the observed changes to potential disease states — such as epilepsy. Using tools such as fitting oscillations & one over f (FOOOF) — an open-source tool for analyzing EEG recordings — we analyzed our results and monitored changes in EEG patterns as well as the correlations among the observed changes to the disease states (14). We confirmed this hypothesis and demonstrated that there are temporal patterns that can be used to classify and sort the different EEG slowing types. We anticipate that future studies will be able to use these methods to correlate specific changes with disease states.

RESULTS

To begin identifying EEG slowing types, we utilized an open-source EEG dataset from Temple University (13). The EEG dataset is comprised of healthy patients and patients with epilepsy, with active seizures occurring throughout the trial. No slowing types were identified prior in the data (which means no labels related to slowing types were included), though slowing was guaranteed at least once in the recording. Since the EEG recordings were preprocessed and annotated, we did not use any type of filter to reduce noise. However, we filtered out EEG channels that had no relevance to our hypothesis. For example, channels located on the right hemisphere of the brain were removed as these channels are prone to exhibit focal slowing naturally and would alter study results. Whether it may be drowsiness, sleep activity, or potential developmental activities in the brain, natural focal slowing can occur (8). Eliminating these channels allowed the machine learning algorithms to solely study the power spectra density (PSD) generated by EEGs without external variables altering the analysis. After analyzing the annotations and establishing which time segments contained slowing based on manual matching of the EEG spike, we analyzed the channels that exhibited no focal slowing or focal slowing. If

analysis occurs over specific channels that contain natural focal slowing, the result from the algorithm classifying data would deviate from what we expect. The International 10–20 system was used to identify the channels that contained focal slowing ("10–20 System EEG Placement," n.d.). The system is a standardized method for positioning EEG electrodes on the scalp.

Knowing that focal slowing naturally occurs in the right temporal region, we removed measuring regions of the brain that had a significant effect on the data to specifically target the abnormal slowing types (15). Next, we plotted the different channels using Matplotlib and FOOOF to evaluate which channels contained the most EEG slowing. The finalized channels FP1, FP2, F3, F4, C3, C4, P3, P4, O1, O2, F7, F8, T3, T5, FZ, CZ, PZ, T1, T2 were utilized for the rest of the study. A periodogram, or MultiTaper PSD, was used to extract the PSD features, which ultimately allowed us to have the power distribution of the frequency as a measure of change in frequency over time. Within an EEG recording, the electrical power of the brain's recorded activity is distributed across different frequency bands, some of which include delta, theta, gamma, etc., which is in the form of PSD. To proceed with analysis using machine learning models, the EEG recording was categorized with three different machine learning algorithms: K-Means, UMAP, and T-SNE. We tested these different algorithms in order to figure out the most efficient and accurate algorithm for clustering the different slowing types.

The first algorithm tested was the K-Means algorithm. The inertia-based graph, a graph that determines how well a dataset was clustered depending on the number of clusters, was necessary to determine the number of clusters required for the intended algorithm. The different clusters sorted different ranges of PSD values that could be attributed to the degree of abnormality of an EEG slowing type. The number of clusters was determined based on analyzing the different inertia-based graphs. We determined that the number of
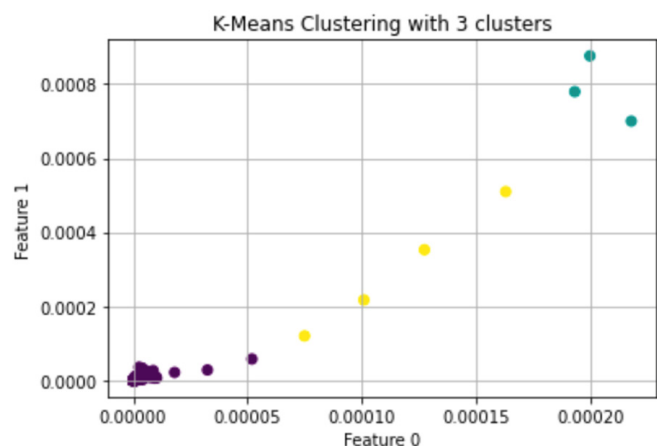

Figure 1: K-Means Clustering. This plot showcases the different clusters in K-Means (n=3) and the three distinct groups of the entire dataset based on the logistical factor PSD. Feature 0 represents time, while Feature 1 represents the power spectra density. The purple describes the base case, which is no slowing, while the other two clusters represent some type of abnormal slowing. The graph primarily takes on the form of an exponential graph to depict the three different clusters adequately without confusion. The silhouette score of the K-Means algorithm was 0.9139.

clusters (k) necessary was 3, as this resulted in low inertia while still minimizing the total number of identified groups. The clusters represent the number of categories the data will be separated into based on the respective PSD values for each time stamp. We applied the K-Means algorithm to the aforementioned calculated PSD values and plotted the results (**Figure 1**). The results showcase three different variants of PSD values. This plot is consistent with our hypothesis, identifying three distinct clusters of the PSD ranges, often attributed to single patient measurement. To test the accuracy of the model, we utilized the Silhouette method to determine the optimal number of clusters in a dataset ("Cluster Quality Analysis Using Silhouette Score," n.d.). Applying the Silhouette method to our K-Means clusters, we received a Silhouette score of 0.914, which is close to 1, demonstrating it is a good score (**Figure 1**).

The same process was applied using the UMAP machine learning approach. According to the within-cluster sum of squares (WSS) metric, we found that the optimal number of clusters for the UMAP algorithm was two (**Figure 2**). The UMAP clustering algorithm resulted in a plot that showcases the two different clusters created by the UMAP clustering algorithm (**Figure 3**). However, upon doing the Silhouette method, the score was around 0.088.

Using the WSS metric on the T-SNE algorithm, we determined the optimal number of clusters to be two (**Figure 2**). The T-SNE silhouette score (0.11524475055798167) was substantially lower than that of K-Means, yet slightly higher than UMAP (**Figure 4**). The T-SNE plot that showcases the different clusters — with respect to the PSD values — identifies how the data performed under two clusters using the respective algorithm (**Figure 1**).

Based on the silhouette scores, we determined that the K-means clustering algorithm was the superior algorithm because of its high silhouette score and distinct clustering of
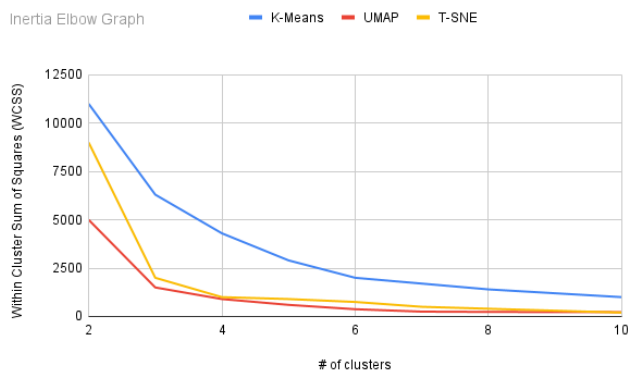

Figure 3: UMAP clustering demonstrates inferior accuracy to that of K-Means clustering. It showcases the different clusters in UMAP clustering, and the two distinct groups of the entire dataset based on the logistical factor power spectra density. The first cluster is marked as purple and Cluster Label "0", and the second cluster is marked as yellow and Cluster Label "1." The Silhouette Score of the UMAP algorithm was around 0.088.

groups. The score for K-means was much higher than UMAP with a percent difference of 90.3% and higher than T-SNE by a percent difference of 87.3%. Once the K-means algorithm was decided upon, we used statistical analysis to ensure that the output we were receiving from the K-means algorithm was producing statistically significant results. After running a t-test on the K-Means graph, the t-statistic was 655.2135148913226, with a p-value of 0.00014. This suggests that our data was being clustered into groups that were significantly different from each other. However, dependency on accuracy was demonstrated later during categorization.

The data we used had time stamps, which indicate periods of the EEG recording. To concisely receive the designated time stamps with the corresponding EEG data, we analyzed the entire dataset with the K-Means machine learning algorithm. Given that the machine learning algorithm separated each individual time segment into a different cluster, the model outputted three different examples of EEG types. Given the three distinct clusters output, based on the data we know that one cluster was specifically designated for no slowing, while the other two contained some type of EEG abnormal slowing. Specifics on what the EEG slowing types were demonstrated later. In the end, we found that the K-Means algorithm was the most successful in clustering the different PSD values from EEG recordings and was able to detect clusters that contained distinct types of EEG slowing.

FOOOF showcases two lines in the recording: one yellow and one green. In the program, FOOOF determines which two channels provide the clearest EEG recordings and showcases the two channels that are closest together within the same region of the brain, which in this case are FP1 and FP2 because they are outputting the cleanest signal (**Figure 5A**). Considering both lines look fairly identical to each other

Figure 2: Cluster-Inertia Elbow Graph. Number of clusters by the Within Cluster Sum of Squares (WCSS) – or Inertia – of all three machine learning algorithms. It assists in distinguishing the appropriate number of clusters. For the K-Means Algorithm, at point 3 there is a greater deviation in numbers between the cluster 2 and cluster 4 than there is with any other cluster, so cluster 3 is the optimal number of clusters. For UMAP, at point 2 there is a greater deviation in numbers between the cluster 1 and cluster 3 than there is with any other cluster, so cluster 2 is the optimal number of clusters. For T-SNE, at point 2 there is a greater deviation in numbers between the cluster 1 and cluster 3 than there is with any other cluster, so cluster 2 is the optimal number of clusters. K-Means also has a greater WCSS value in comparison to the other algorithms, which is an indication of greater variability of the observations within the cluster.
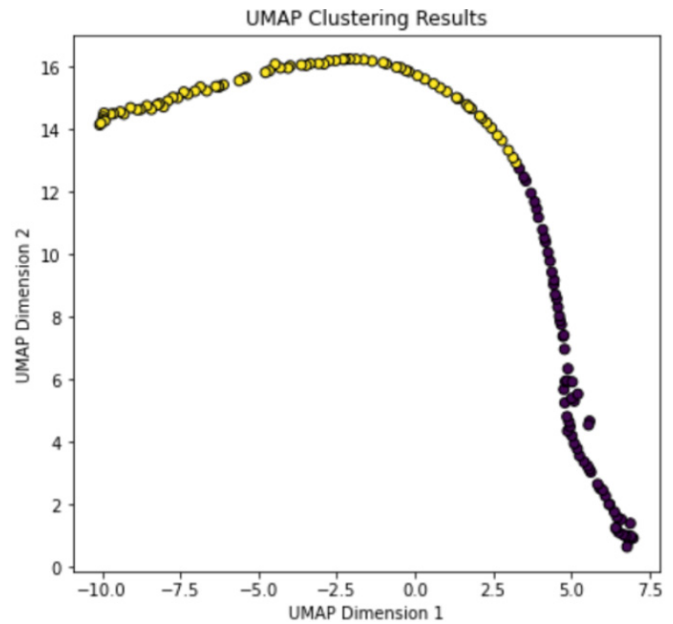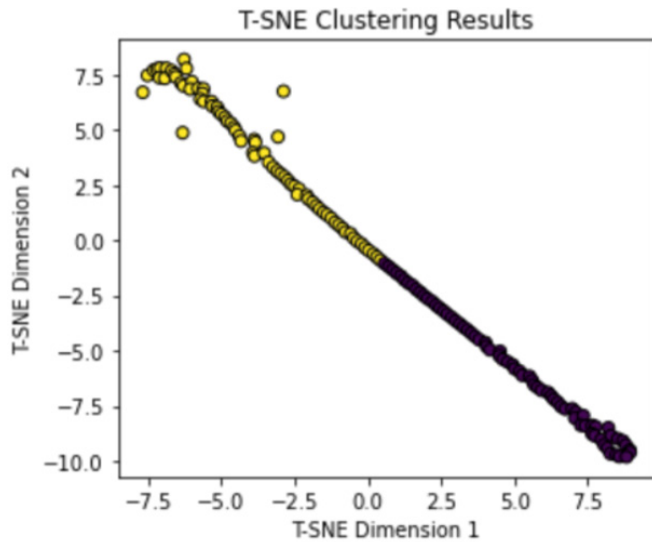
T-SNE Clustering Results

Figure 4: T-SNE clustering demonstrates inferior accuracy to that of K-Means clustering. This plot showcases the different clusters in T-SNE clustering, and the two distinct groups of the entire dataset based on the logistical factor PSD. The Cluster Label "1," marked as yellow, demonstrates the first cluster, while the Cluster Label "2," marked as dark purple, demonstrates the second cluster. All other cluster numbers within the range are not represented because there is no cluster at that point. The silhouette score of the T-SNE algorithm was reported as ~0.115.

in terms of slowing examples, it can be concluded that such an EEG recording is accurate and can be used for visual analysis. After visualizing the EEG clusters in FOOOF, the following was extracted.

The baseline sample is the sample that contains all the other 10-second intervals. This period does not experience any type of harmful/abnormal slowing (or any slowing in general) and will ultimately be disregarded completely as a deviated slowing type. In other words, this is an example of no slowing, which does not demonstrate any nebulous outcomes. This was classified as a baseline during the K-Means analysis **(Figure 5A)**.

The next case demonstrates another variant of EEG slowing. It showcases a similar pattern of dropping/caving downward due to slowing **(Figure 5B)**. Such can be associated with triphasic waves, given the nature of such a structure. Case one is shown, which is an example of Postictal/Focal slowing in Epilepsy **(Figure 5B)**. Case two is shown, which is an example of simple Triphasic slowing that can still be attributed to degenerative diseases **(Figure 5C)**.

The last case showcases a different type of slowing — generalized slowing — specifically mild generalized slowing — given that it contains a slowed PDR and a poor AP gradient, as can be demonstrated through the structure of the waves. When a frequency is labeled at a much lower amplitude and faster frequency than other readings around it, it will automatically contain a poor AP gradient and yield the possibility of containing EEG slowing. This type of slowing is typically from a type of sedative or medication (as mentioned in previous sections) and would thus be differentiated from an abnormal EEG slowing reading. The following can be displayed through the last two trials of 10-second data **(Figure 5D)**.

DISCUSSION

Thorough analysis of both the machine learning results and the real-time EEG data from the FOOOF program provided evidence that power spectra play a substantial role in EEG slowing recordings and exhibit a potential correlation with the phenomenon of EEG slowing, based on not only the outputs we received from clustering but also on the real-time EEG data correlated to distinct waveforms. Upon determining the most suitable machine learning algorithm based on silhouette scores, we categorized the data into
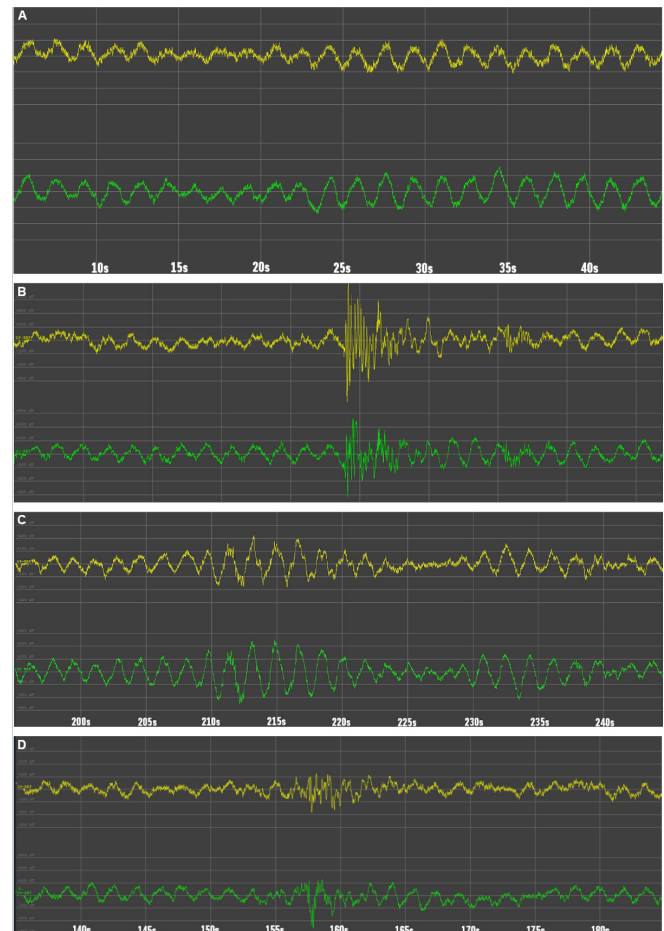

Figure 5: EEG recordings. A) Base case EEG recording. The data are smooth and symmetric with no notable variations during the trials and no difference in AP gradient or PDR. A deviation in AP gradient would indicate a reading abnormality, such that lower amplitude and faster frequencies are seen in anterior derivations with higher amplitude and slower frequencies in posterior derivations. **B)** Classic example of EEG recording in slowing formation. The waveform is initially normal, but the symmetry and normality is disrupted for ~7-8 seconds when the amplitude of the wave shifts to double, then half of the original, and the wavelength markedly contracts. A common example of a neurodegenerative disorder with similar EEG readings is epilepsy. Postical slowing shows abnormal EEG readings similar to this example. **C)** EEG recording in deviated slowing formation. Showcasing the ~3-minute mark, the graph curves inward and in a concave-in type structure, indicating some sort of slowing occurring in the region in contrast to the other events. This is a clear example of triphasic slowing, an abnormal waveform. **D)** EEG recording of generalized slowing. This graph showcases the first 7-10 minutes of the EEG recording. Both graphs demonstrate a poor AP gradient and lower amplitude in signal, demonstrating generalized slowing.

different cases. Since the data in the study is unsupervised, it is impossible to understand the "accuracy" of the model. However, the Silhouette score gives us a similar output in that it tests the correctness of the PSD differentiation per cluster by measuring how well each cluster is defined, evaluating both how closely data points within a cluster are grouped (cohesion) and how distinct they are from points in other clusters (separation). In the future, we plan on creating some sort of accuracy checkpoint in which we may go back and look at the clusters and re-assign all of the headers so an accuracy percentage can be outputted. Each cluster represented a distinct type of EEG slowing — various abnormal types and no EEG slowing — though the specific characteristics remain unknown. Some data examples contained segments of slowing, while others were categorized as the baseline case (which is no slowing). As per the study's nature, we anticipated that only certain cases would manifest EEG slowing while others would remain consistent with the baseline. The power spectra exert a significant influence on the categorization of EEG slowing, showcasing how an abnormal EEG slowing type has a significantly different PSD value in contrast to a normal EEG slowing type and the baseline, suggesting the potential for further insights.

Using the three different machine learning algorithms and comparing not only the Silhouette scores but also the t-test and p-value, it is possible to come up with a potential accuracy detector. Initially comparing the silhouette scores of each of the three distinct machine learning algorithms, the silhouette. By analyzing the different silhouette scores, it is apparent that the clusters in K-Means were performing much more effectively than the other machine learning algorithms and therefore the K-means was the most accurate model to use in this study. K-Means, in the context of this study, is primarily an algorithm dedicated to partitioning and separating the data into distinct clusters. In contrast, both T-SNE and UMAP are solely dedicated to preserving the local or global structure of high-dimensional data in lower-dimensional embeddings for visualization purposes. This study does not require the local and/or global structures of the high-dimensional data to be preserved and is instead focused on separating the data into distinct clusters, which is exactly what the K-Means algorithm is designed to do. To this end, we pre-processed the data by selecting specific channels, thereby reducing the dimensionality of the data. This reduction in dimensionality decreases the need for techniques like UMAP and T-SNE, making K-Means a more suitable choice for clustering in this context.

Our categorization reveals that all non-baseline cases — clusters one and two demonstrating abnormal EEG slowing types — exhibited some form of EEG slowing. This finding implies that all cases not classified as baseline were, in fact, a variation of EEG slowing, opening up new avenues for early detection in the context of EEG slowing based on the PSD value associated with the data.

Based on the initial ten seconds, some slowing occurred in the prefrontal cortex. Upon further analysis, we labeled it as intermittent rhythmic delta activity given the nature of the wave curving inwards, along with the shape of the overall wave. Slowing examples sometimes have random dips that immediately return to their original state, such as those that occurred within the initial 10 seconds.

Our primary focus remained on EEG slowing due to its direct impact on degenerative diseases like Alzheimer's (7). Understanding the fundamental connection is imperative for devising treatment strategies. However, this study can readily expand to encompass other attributes correlated with PSD, provided that the underlying mechanism remains unchanged and no additional variables are introduced. For example, analyzing the rate of slowing based on the power in the signal or expanding the study to look at spatial characteristics may be a viable indicator for categorizing the different EEG slowing types.

Currently, in this study, we have found that one of the classified examples has been attributed to epilepsy. As demonstrated, the clear repetitive peaks resemble the form of an EEG slowing activity type, yet the specific type is unknown (**Figure 6**). However, considering it is relatively spaced out with higher peaks — in contrast to the other peaks in the recording — it is a clear indication of EEG slowing. After looking at the waveforms of an epileptic event, it appears that a form of epilepsy does show the same type of EEG-slowing activity that we see in our dataset (17). The same spaced-out waves with higher peaks resemble an EEG-slowing activity type similar to that of occipital intermittent rhythmic delta activity. Although only one recording was tested and classified, it suggests that PSD characteristics and categorization do indeed have an influence over classifying neurodegenerative diseases, like epilepsy, and suggests these characterizations can be efficient and accurate. Other studies, especially those that have specifically analyzed the different EEG slowing types in neurodegenerative diseases such as Alzheimer's, found that even Alzheimer's exhibits a different EEG slowing type, showcasing an increased relative theta power (7). Increased relative theta power is additionally correlated with EEG slowing types, yet a specific EEG slowing type is yet to be found. With the findings in our study, we hope to continue on the classification of different EEG slowing types, with the hope of attributing distinct neurodegenerative diseases with specific EEG slowing types/characteristics.

This current study relies on the reliability of the data received by Temple University in its collection of EEG data. Given that the data did not contain any labels indicating EEG slowing, determining whether the machine learning algorithm was adequate for the situation was abstract and nebulous — one that poses a limitation in our study. Additionally, this study analyzes three different machine learning algorithms, but there may be other algorithms that could serve as more accurate and efficient.

In conclusion, we can confidently assert that power spectra are a fundamental attribute related to EEG slowing and exhibit a direct correlation. Taken together, these results confirm our hypothesis that there are fundamentally key distinctions between the types of EEG slowing, including temporal characteristics. Furthermore, the machine learning algorithm-based approach employed in this study is versatile and can be adapted to classify other EEG patterns or neurological features, such as different types of brain wave abnormalities or seizure activity, with appropriate adjustments to the model parameters and input variables.

MATERIALS AND METHODS

All data utilized in this research were sourced from the Temple University Electroencephalography (EEG) Resources (13). This dataset comprises approximately 27,000 clinical

EEG recordings from various patients collected at the Temple University Hospital (TUH). The data gathered through this trial was pre-annotated with details such as disease type showcased, type of patient, etc. by trained electrophysiologists. The data collection spans a diverse range of patients, particularly those with epilepsy. It also includes those without physical or mental impairments, serving as control subjects. Each individual consented accordingly to the IRB (13).

Patients involved in the study were recruited upon admission to one of the hospitals on the Temple University grounds. Each patient underwent assessments for various diseases — including regular day-to-day tasks, sleeping, and regular bodily function — and various electrodes were placed on their heads to record EEG samples. These samples allowed for further analysis. Patients were diagnosed with multiple diseases, including epilepsy, delirium, Alzheimer's, and general slowing. Daily screenings were conducted to update study results continuously, and the study itself, including the data collection and methods utilized, was updated daily to maximize results for data analysts. Another corpus — a subset within the same dataset — tested an equal split between those diagnosed with epilepsy and those without any mental impairment, with 100 patients each.

EEG Analysis

EEGs were recorded within a clinical setting and intense supervision, as per the Temple University protocols. All EEG recordings used throughout the session had a sampling rate of 250 Hz and a 19-channel montage with ground and reference electrodes placed according to the international 10-20 system.

All EEG traces and recordings have been preprocessed and annotated during production. Each time an EEG sample was recorded and issued, the readings were annotated based on whether slowing was present, whether any seizures occurred, general time stamps of recordings, and other logistical factors. The two crucial files used in this study are labeled "LBL" and "TSE" files. The TSE file includes term-based annotations — annotations based on a particular segment of time. The LBL file includes event-based annotations — annotations focused on identifying individual events or occurrences within the EEG data — using all available seizure types.

The LBL file contains the following three fields: version number, montage mlock, and level block. Levels are used to create a hierarchical structure, with sublevels used to track data, such as iterations or sources. For the specific dataset we are using, one level and one sublevel are used for seizure annotations. These levels describe the label used for each annotation.

The TSE file showcases information crucial for classification purposes. As it is time-synchronized, it can be utilized during time-series analysis. In this file, the following fields are present: the start time in seconds, the stop time in seconds, the annotation label, and the probability of the label. These fields are necessary for the EEG slowing readings and reports, enabling further analysis.

For visualization purposes, we used EPViz, an EEG Prediction Visualizer developed by the Johns Hopkins Whiting School of Engineering, in the Neuro Systems Analysis Laboratory. This tool allowed us to view the PSD on each channel and observe its live reaction on these EEG slowing files.

Knowing that the duration of an EEG event episode is 10 seconds long and there are 144 episodes based on the information provided by Temple University, EEG recordings were a maximum of 1440 seconds. This number can be variable depending on the number of episodes in the EEG recording. We looped through all of the 10-second segments in the 1440-second data and recorded the computed PSD values. Each PSD's average values were added to a pandas data frame with final dimensions (399 x 144).

Alongside power spectra analysis, other examples of analysis are provided, as the EEG data underwent quantitative analysis, including exporting the clinical recordings in European Data Format and further importing them into Spyder Magnetoencephalography (MNE)-Python for preprocessing. At this point, Matplotlib was utilized to create plots for understanding the time series analysis.

All data were preprocessed in MNE. The variable explorer and other built-in functions were used to calculate the PSD for the project. Once values were calculated and sorted on the different trials, a Pandas data frame and conversion into a CSV file were completed in order to process and analyze the data further.

Frequency Domain Analysis

The frequency domain operates by analyzing the power spectra, which illustrate the frequencies of each EEG recording and the distribution of each frequency. For instance, one EEG recording may exhibit more delta activity than alpha activity. FOOOF is an open source tool for analyzing EEG recordings, showcasing a variable number of periodic components with specific characteristics like center frequency, power, and bandwidth. It distinguishes peaks in power spectra without predicting bonds or intervals while accounting for the aperiodic component. We used FOOOF to quantitatively measure each EEG slowing recording with power spectra. For instance, increased delta theta in the power spectra, between 1 and 4 Hz and 3.5 to 7.5 Hz, usually indicates cognitive impairments, and it is plausible to use the power spectra to understand the thresholds between the different versions of slowing.

Time-Frequency Analysis with MNE

In addition to pre-processing, we also used MNE for time-frequency analysis. In addition to the frequency domain technique, time-frequency analysis also uses the spectral content to further analyze the data. Additionally, MNE also allowed for the analysis of PSD, which represents the power distribution of EEG series in the frequency domain. However, there is an additional section for time-frequency analysis, in which we can read the epochs and analyze each epoch's start and stop times. We can look at the stimulus period and even analyze the different conditions performed during that same period. As established through the TSE file, the start and stop times for each slowing have been indicated. Using this information, the time-frequency was analyzed and particularly interesting features, such as PSD, were noted.

Frequency-Domain Clustering

This type of method is specialized in EEG analysis which involves grouping different types of EEG data based on similarities in their frequency characteristics. in this context, it would be focusing on the PSD. PSD is calculated using methods like the Fourier transform and provides critical

insights into EEG slowing. Specifically, in this context, clustering happens when it extracts particular features from extraction in the PSD, where relevant frequency-specific features are identified, such as power in specific bands or ratios between bands. These features may be further processed using dimensionality reduction techniques like UMAP or t-SNE to manage the high-dimensional nature of EEG data (more on that in the later sections). Frequency-domain clustering has numerous applications, including for predictive measures when it comes down to neurological degenerative diseases such as epilepsy and Alzheimer's, as well as distinguishing cognitive characteristics such as what type of slowing is present in the mind. Tools like EEGLAB, FieldTrip, and Python libraries such as MNE-Python and scikit-learn are commonly used for analyses, but machine learning algorithms have a more practical application given the variables at hand.

Time Domain Clustering

This type of clustering in EEG analysis focuses on grouping data based on the temporal characteristics of the EEG signals. This approach examines the raw EEG waveforms or features derived directly from the time domain, such as signal amplitude and latency, to identify clusters that correspond to different brain states or conditions (18). In this context, time-domain clustering is particularly useful for detecting temporal patterns like oscillations, spikes, or other transient events in the EEG signal (especially when analyzing PSD values and seeing if there are outliers or spikes within time), which may be related to various cognitive processes or neurological conditions. The process typically involves extracting relevant time-domain features and may include dimensionality reduction to manage the high-dimensional nature of EEG data. Time-domain clustering can be applied to tasks such as detecting epileptic spikes or classifying sleep stages based on time-domain signal characteristics. However, challenges include handling noise and artifacts, selecting appropriate time-domain features, and ensuring the quality and validity of the clusters. Tools such as EEGLAB, FieldTrip, and Python libraries like MNE-Python and scikit-learn are commonly used for this type of analysis, enabling researchers to explore the temporal dynamics of EEG data. Additionally, machine learning algorithms such as K-Means Clustering for general clustering would accurately be used in this situation. Furthermore, if a dimensionality reduction technique is utilized, options such as UMAP and T-SNE would adequately fit (mentioned and explained in detail in later sections).

Machine Learning Algorithms

Clustering is the process of grouping similar data points based on some type of feature, which could be in the form of a computational characteristic of some sort. In this study, three different machine learning clustering algorithms were implemented: K-Means, UMAP, and T-SNE. As mentioned above, due to the fact that both UMAP and T-SNE were tailored towards time domain clustering and were thus depicted as the optimal solution for performing machine learning analysis upon the PSD values, utilizing all three methods was necessary in order to determine the optimal algorithm. K-means clustering is a machine learning algorithm dedicated to grouping a certain number of "n" observations

into K-clusters ("What Is Clustering?", n.d.). In order to determine the optimal clusters in the study, analyzing an inertia-based graph provides optimal results. Using the built-in "optimize_k_means" function, we visualized the inertia-based graph for the data **(Figure 1).** The graph outputs how well the data is being clustered based on "n" number of clusters, and the optimal number of clusters is the peak. Inertia typically measures how well a dataset was clustered by K-Means by calculating the distance between each data point and its centroid, squaring this distance, and summing these squares across one cluster. Given that the data provided in our study contained no labels, K-Means Clustering was a suitable choice, given that K-Means Clustering is considered an unsupervised learning algorithm. This algorithm was implemented in Python, Jupyter Notebook, and utilizes a multitude of libraries including Pandas and StandardScaler for practical applications. As previously mentioned, T-SNE and UMAP were utilized.

UMAP can be used to cluster high-dimensional data (20). UMAP heavily focuses on local features. Additionally, UMAP clusters on an epoch-by-epoch basis and additional analysis on the different stages of slowing could potentially commence using the different cohorts pulled from the dataset. In this case, we use UMAP to visualize the average value per cohort of the power spectra and classify the different groups according to three different distinct ranges. All outliers, such as outputs from the channels that were removed, were removed prior due to the preprocessing done in MNE (since they would have deviated from the results). T-SNE is an alternative to UMAP since it is also a clustering algorithm that could potentially be used during our trials. UMAP can also be used to analyze time domain clustering and its impact on the temporal characterization of EEG slowing. This technique is primarily unsupervised but does contain supervised attributes or steps in the algorithm. The algorithm operates as follows. The first step is projection, which is the process or technique of reproducing a spatial object upon a plane, a curved surface, or a line by projecting its points. The second step is approximation, where the algorithm assumes we only have a finite number of data samples (points), not the entire set. The third step is manifold, which is a topological space loosely resembling Euclidean space near each point. The fourth step is uniformity. The uniformity assumption tells us if our samples are uniformly distributed across the manifold. In this process, a dimensionality reduction technique assumes the available data samples are evenly distributed across a topological sphere that can be approximated from these finite data samples and mapped to a lower dimensional space. While UMAP is used in both the Time Domain and Frequency Domain, the Frequency Domain only focuses on the local region, while Time Domain Analysis focuses on both local and global structures.

Another method to visualize high-dimensional data in a low-dimensional space using a nonlinear dimensionality reduction technique is t-SNE. This is an unsupervised model and is additionally considered nonlinear in its filtering and funneling processes. t-SNE works initially to compute the similarities between all the data points based on their high-dimensional feature representations computed by the Gaussian distribution. Then, it constructs conditional probability distributions for all high-dimensional data points, creating a distribution representing the similarity between

that point and all other points in the high-dimensional space. It next creates a similar distribution, but this time in lower dimensionality — either in 2D or in 3D. Finally, in the end, it minimizes the divergence, adjusting the locations of data points in the lower-dimensional space to minimize the divergence between the high-dimensional conditional distributions and the lower-dimensional similarity distributions. This can be done using gradient descent optimization. After all these processes, it finishes with the classification phase, also used in this research paper to test accuracies.

Machine Learning Silhouette Score

To assess the accuracy of the machine learning model, it is critical to apply an accuracy test to the output. In machine learning, most models attempt to test accuracy by analyzing the labels and ensuring that the output of the model is matching with the labels. In this study, the silhouette score was used as our accuracy model. The silhouette score is a metric used to evaluate the quality of clusters in a clustering analysis. It measures how similar an object is to its own cluster compared to other clusters, providing a silhouette score that helps identify the most suitable number of clusters by maximizing cohesion within clusters and minimizing their overlap. The silhouette score helps assess how well-separated the clusters are and how well each data point is assigned to its corresponding cluster.

The silhouette score was calculated in four steps. For each of the data points, we calculated the Euclidean distance between that data point and all other data points in the nearest cluster that the data point does not belong to, known as the inter-cluster distance. This measures how dissimilar the data point is to points in specific neighboring clusters. We then calculated the average distance between the data point and all other data points within the cluster. This measures how similar the data point is to other points within its cluster, known as the intra-cluster distance. At this point, the silhouette score was calculated based on the following formula:

$$score = \frac{(intracluster\ distance) - (intercluster\ distance)}{(intercluster\ distance, intracluster\ distance)}$$

The value of the score ranges from -1 to +1, where the positive value indicates that the data point is well-matched to its cluster and poorly matched to neighboring clusters, and the negative value indicates that the value was probably assigned to the wrong cluster. To compute the overall quality of the clustering, the silhouette scores of all data points are averaged. A higher average silhouette score indicates that the clusters are well-separated and appropriately assigned.

REFERENCES

1. National Institute on Aging (n.d.). "Alzheimer's and Dementia." National Institute on Aging, n.d. https://www.nia.nih.gov/health/alzheimers-and-dementia.
2. Smith, S. J. M. "EEG in Neurological Conditions Other than Epilepsy: When Does It Help, What Does It Add?" *Journal of Neurology Neurosurgery & Psychiatry*, vol. 76, suppl. 2, 2005, pp. ii8–ii12, https://doi.org/10.1136/jnnp.2005.068486.
3. Mayo Clinic (n.d.). "EEG (Electroencephalogram)." Mayo Clinic, 11 May 2022. Accessed 5 May 2024.
4. Nayak, Chetan S., and Arayamparambil C. Anilkumar. "EEG Normal Waveforms." StatPearls, StatPearls Publishing, 24 July 2023.
5. Soikkeli, Raija, et al. "Slowing of EEG in Parkinson's Disease." *Electroencephalography and Clinical Neurophysiology*, vol. 79, no. 3, Sept. 1991, pp. 159–65, https://10.1016/0013-4694(91)90134-p.
6. Popa, Livia Livint, et al. "The Role of Quantitative EEG in the Diagnosis of Neuropsychiatric Disorders." *Journal of Medicine and Life*, vol. 13, no. 1, Jan. 2020, pp. 8–15, https://10.25122/jml-2019-0085.
7. Benz, Nina, et al. "Slowing of EEG Background Activity in Parkinson's and Alzheimer's Disease with Early Cognitive Dysfunction." *Frontiers in Aging Neuroscience*, vol. 6, no. 314, Nov. 2014, p. 314, https://doi.org/10.3389/fnagi.2014.00314.
8. St. Louis, Erik K. "The Abnormal EEG." Electroencephalography (EEG): An Introductory Text and Atlas of Normal and Abnormal Findings in Adults, Children, and Infants [Internet]. U.S. National Library of Medicine, Accessed 1 Jan. 1970.
9. St. Louis, Erik K. "EEG in the Epilepsies." Electroencephalography (EEG): An Introductory Text and Atlas of Normal and Abnormal Findings in Adults, Children, and Infants [Internet]. U.S. National Library of Medicine, 1 Jan. 1970. Accessed 5 May 2024.
10. Nardone, Raffaele, et al. "Usefulness of EEG Techniques in Distinguishing Frontotemporal Dementia from Alzheimer's Disease and Other Dementias." *Disease Markers*, vol. 2018, Sept. 2018, https://doi.org/10.1155/2018/6581490
11. "Machine Learning, Explained." MIT Sloan, 21 Apr. 2021,
12. Yoo, Kyoung-Seok. "Motion Prediction Using Brain Waves Based on Artificial Intelligence Deep Learning Recurrent Neural Network." *Journal of Exercise Rehabilitation*, vol. 19, no. 4, Aug. 2023, pp. 219–227, https://doi.org/10.12965/jer.2346242.121.
13. Picone, Joseph. "Electroencephalography (EEG) Resources." Temple University EEG Corpus Downloads. Accessed 5 May 2024.
14. Donoghue, Thomas, et al. "Parameterizing Neural Power Spectra into Periodic and Aperiodic Components." *Nature Neuroscience*, vol. 23, no. 12, Nov. 2020, pp. 1655–1665, https://doi.org/10.1038/s41593-020-00744-x
15. Benbadis, Selim R., MD. "Focal (Nonepileptic) Abnormalities on EEG." *Medscape*, 16 Jan. 2024. Accessed 5 May 2024.
16. Shahapure, K. R., and C. Nicholas. "Cluster Quality Analysis Using Silhouette Score." 2020 IEEE 7th International Conference on Data Science and Advanced Analytics (DSAA), Sydney, NSW, Australia, 2020, pp. 747–748, https://doi.org/10.1109/DSAA49011.2020.00096.
17. LaBarbera, Vincent, and Duyu Nie. "Occipital Intermittent Rhythmic Delta Activity (OIRDA) in Pediatric Focal Epilepsies: A Case Series." *Epilepsy & Behavior Reports*, vol. 16, Jan. 2021, p. 100472, https://doi.org/10.1016/j.ebr.2021.100472.
18. Javed, Ali, et al. "A Benchmark Study on Time Series Clustering." *Machine Learning with Applications*, vol. 1, Sept. 2020, p. 100001. https://doi.org/10.1016/j.mlwa.2020.100001.

19. "What Is Clustering? | Machine Learning." Google, Google Developers. Accessed 5 May 2024.
20. McInnes, Leland, et al. "UMAP: Uniform Manifold Approximation and Projection." *The Journal of Open Source Software*, vol. 3, no. 29, Sept. 2018, p. 861, https://doi.org/10.21105/joss.00861.